

Different kinds of long-term variability from Cygnus X-1

S. Benlloch*, K. Pottschmidt^{†**}, J. Wilms*[‡], M.A. Nowak[§], T. Gleissner* and G.G. Pooley[¶]

*IAAT – Astronomie, Sand 1, 72076 Tübingen, Germany

[†]MPE, Giessenbachstr. 1, 85748 Garching, Germany

**ISDC, Ch. d'Écogia 16, 1290 Versoix, Switzerland

[‡]Department of Physics, University of Warwick, Coventry CV4 7AL, UK

[§]MIT/CSR, Cambridge, MA 02139, USA

[¶]Cavendish Laboratory, Madingley Road, Cambridge CB3 0HE, UK

Abstract. We present a study of the long-term variability of Cyg X-1 using data from the RXTE/ASM and the RXTE/PCA during the time between the two soft states of 1996 and 2001/2002. This period has been characterized by many short ASM flaring episodes which we have identified as "failed state transitions". The 150 d period which has been seen before and shortly after the 1996 soft state is not obviously present in the ASM rate during most of this time. Applying selection criteria from our pointed RXTE/PCA observations to exclude the flaring episodes we show that the 150 d period can indeed still be significantly detected in the hard state. Furthermore, while the ~ 420 d timescale associated with the flaring is reduced in the selected hard state count rate, it is still pronounced in the temporal evolution of the corresponding hardness ratios. The Ryle radio flux is also consistent with the 150 d period being present but distorted during this time.

INTRODUCTION & SELECTION CRITERIA

Historically several different scales of long-term variability in Cyg X-1 have been reported. Multiwavelength observations (optical, radio, hard and soft X-ray) between 1996 and 1998 established that a 150 d signature is the dominant variability timescale which is suggested to be caused by precession and/or radiative warping of the accretion disk [1, 2]. Recently this period has also been confirmed with earlier Ginga data [3]. From 1998 onwards, however, this signature is not obvious in the soft X-ray flux anymore (Fig. 1, upper panel): Although mainly in the hard state, Cyg X-1 has been more active since before, i.e., more flaring episodes during which the source can be found in the intermediate state (=failed state transitions [4]) – sometimes even reaching the soft state – have been observed. This goes together with a sharp and significant change in the properties of the short-term variability in June 1998 [4]. Oezdemir and Demircan [5] suggested to avoid the distortion of the possible periodicities in the original data introduced by the high/soft state and the failed state transitions by truncating the RXTE/ASM lightcurve at 30 cps (threshold derived from visual inspection). They report a clearer detection of the 150 d period in the 1996 to 1999 ASM data. Based on the principal idea of selecting only hard state

data, we:

- perform a period search for RXTE/ASM data dominated by the flare-distorted phase from 1998-2001,
- use physical selection criteria derived from monitoring Cyg X-1 with RXTE/PCA since 1998,
- use two statistics for unevenly sampled data (Lomb-Scargle PSD and epoch folding),
- also study the variability of the RXTE/ASM colours.

Our selection criteria (lower panels of Fig. 1) are based on the photon index Γ of the PCA spectra and the time lags (between the 2–4 and 8–13 keV flux), since they have been shown to be good diagnostics for failed state transitions [6, 7]. Γ and lag are interpolated from the PCA sampling to the ASM sampling. In detail the states are defined as follows: (i) the canonical hard state is characterized by hard PCA spectra with $\Gamma < 2.1$, (ii) spectra with $2.1 \leq \Gamma \leq 2.4$ are typical for failed state transitions, and (iii) for the softest spectra with $\Gamma > 2.4$, enhanced time lags ≥ 5.3 ms also point towards a failed state transition, while "normal" time lags < 5.3 ms characterize the soft state.

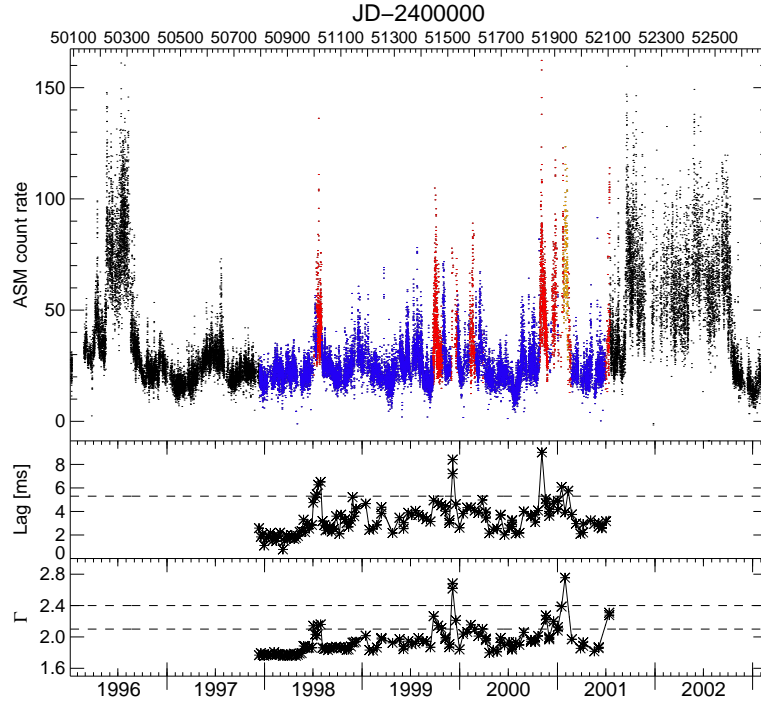


FIGURE 1. Upper panel: RXTE/ASM 1.3–12.2 keV lightcurve of Cyg X-1. A categorization of the ASM data points into different states has been performed using the parameters and selection criteria displayed in the two lower panels: the parameters have been derived from regular monitoring observations of Cyg X-1 with the RXTE/PCA and consist of the Fourier time lag between the 2–4 keV and 8–13 keV high resolution lightcurves (middle panel) as well as of the spectral photon index Γ (lower panel). See text for an explanation of which selection criteria (horizontal lines) apply for which state.

LONG-TERM VARIABILITY, SIGNIFICANCES

Fig. 2 shows the Lomb-Scargle periodogram [8, 9] for all ASM data between 1997 December and 2001 July. The analysis of the total count rate as well as of the three ASM sub-bands is displayed. Prior to the analysis, the lightcurves have been rebinned to a 7 d resolution in order to avoid aliases due to the 5.6 d orbital period. The dashed lines represent the 99.9% “local significance” levels for a set of 5000 Monte Carlo white noise simulations (for more details on the significance determination see [10]). As expected, the 150 d signature is not significantly present in the overall ASM data. Longer timescales seem to be more prominent especially a broad peak around 420 d (of course, increasingly fewer cycles are covered). However, there is already an indication here that the 150 d period is still present from the data in the 5–12 keV energy band, also strengthening the idea of possible inner disk / radio jet coupling.

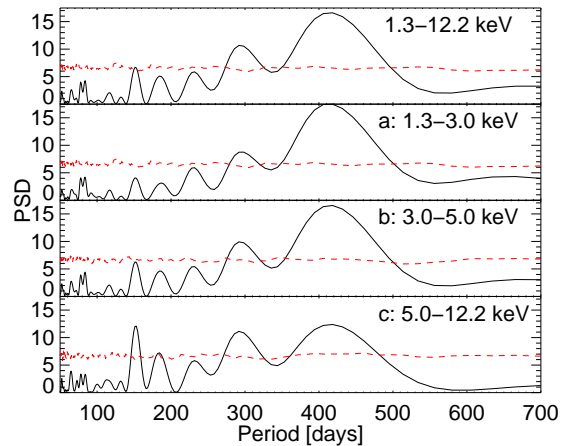


FIGURE 2. Lomb-Scargle periodogram of all Cyg X-1 ASM data from 1997 December to 2001 July. No state selection criteria have been applied. The first panel shows the result for the full ASM energy range while the other three panels are derived for the indicated sub-bands.

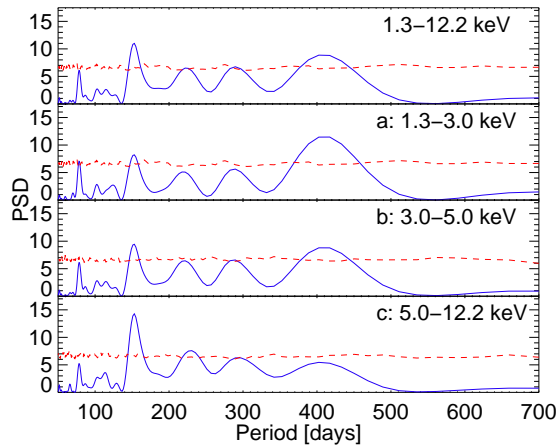


FIGURE 3. The same as Fig. 2 but for the hard state selected ASM data only.

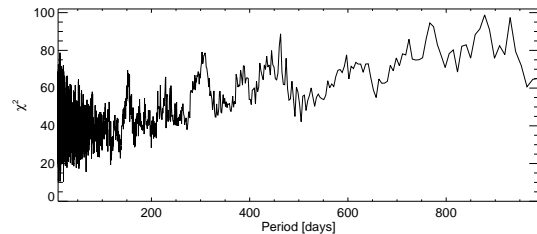


FIGURE 4. Results of a period search for the hard state selected ASM data using the epoch folding method.

IS THE 150D SCALE STILL THERE?

After applying the selection criteria described above to keep only the hard state data, two types of changes are apparent from the resulting Lomb-Scargle PSDs (Fig.3): the significance of the 150d period increases in all energy bands and it can now be significantly detected in the total count rate. In parallel the opposite behavior is displayed by the 420d component: compared to the unselected dataset its significance decreases in all energy bands, most strongly in the hardest band where it decreases below the given significance level. These two trends lead to the 150d signature being the most prominent timescale of the total ASM rate in the cleaned hard state. Its presence is also confirmed by the results of an epoch folding period search, see Fig.4.

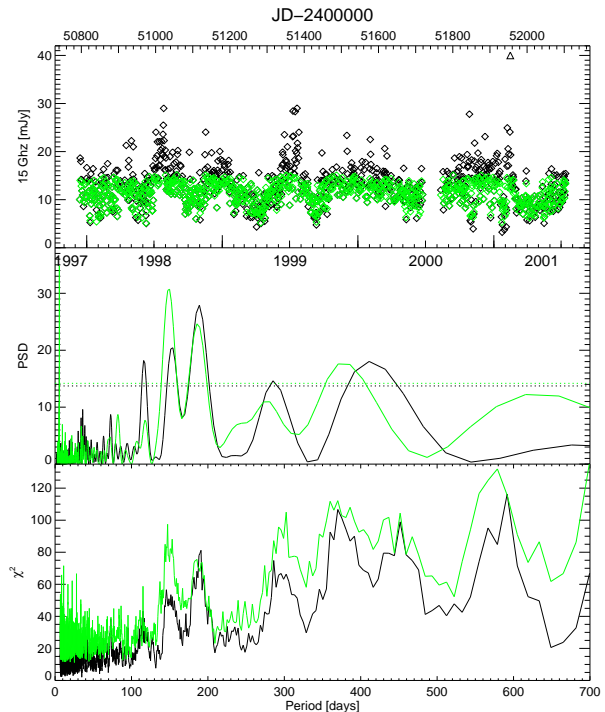


FIGURE 5. Upper panel: 15 GHz radio lightcurve measured by the Ryle telescope. The full data set (dark symbols) as well as the hard state selected one (light symbols) is shown. See text for details on the flux selection criterion applied in this case. Middle panel: Lomb-Scargle PSDs for the Ryle lightcurves. Here the 99.9% “global significance” levels are shown since they are not expected to deviate from the local significances. Bottom panel: Epoch folding analyses for the Ryle lightcurves.

CONFIRMATION FROM THE RADIO FLUX

While the analysis of the overall 15 GHz radio lightcurve – performed over the same time interval as the ASM analysis – does show the presence of the 150d signature as a formally significant timescale, other nearby timescales arise with comparable significance (Fig. 5, dark symbols and lines). Since we are studying a non-canonical hard state (changed short-term X-ray variability [4]) it is not a priori clear that a selection based on the X-ray states is also appropriate for the radio emission – although the tendency for radio flaring during failed state transitions is known. In this first approach we thus use a flux selection criterion ($5 \text{ mJy} < \text{Ryle flux} < 15 \text{ mJy}$) and find that it helps to better work out the 150d timescale (Fig. 5, light symbols and lines). The overall picture of the 150d period being present but buried by the flaring activity is thus consistent. However, from this radio dataset alone and using the preliminary flux selection criterion one could not determine the physical reality of the

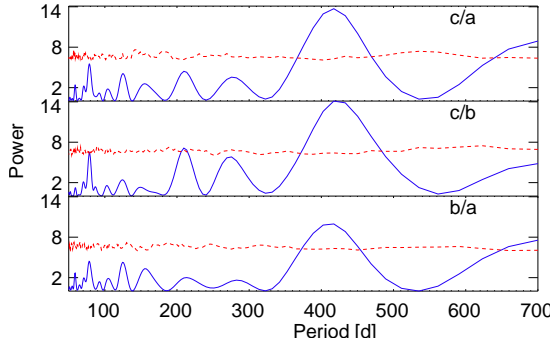


FIGURE 6. Lomb-Scargle periodogram of the colours derived from the hard state selected ASM data. The energy bands a, b, c used for the colour ratios are defined in Fig. 2).

150 d period as compared to, e.g., the 190 d variability. Note that a 1d-binned-lightcurve was analyzed here – leading to the presence of the 5.6 d orbital period in the PSD – and that the described effects are also present using 7d-bins, but are less pronounced.

A DIFFERENT SPECTRAL TIMESCALE?

It is also interesting to perform the same period search on the ASM colours, applying the hard state selection criteria (Fig. 6): the 150 d period is not visible at all, while the 420 d timescale is clearly dominating. We cautiously suggest that while the 150 d period is a pure intensity variation, there might be another characteristic timescale driving the soft X-ray flux, associated with spectral changes. Note that this is true even after removing the failed state transitions themselves.

ACKNOWLEDGMENTS

This work has been financed by DLR grant 50 OX 0002 (SB) and by DFG grant Sta 173/25-3 (KP, TG). KP acknowledges support from Chandra grant GO-4050B and from the Société Suisse d’Astrophysique et d’Astronomie for enabling her to attend the “X-Ray Timing 2003: Rossi and Beyond” conference in order to present this work. The co-authors dedicate the presentation of this work to the twins, Eric and Marvin, who timed their birth allowing their mother (SB) to finish the analysis but suggesting that its presentation should be done by one of the collaborators (KP).

REFERENCES

1. Pooley, G. G., Fender, R. P., and Brocksopp, C., *MNRAS*, **302**, L1 (1999).
2. Brocksopp, C., Fender, R. P., Larianiov, V., Lyuty, V. M., Tarasov, A. E., Pooley, G. G., Paciesas, W. S., and Roche, P., *MNRAS*, **309**, 1063 (1999).
3. Kitamoto, S., Egoshi, W., Miyamoto, S., Tsunemi, H., Ling, J. C., Wheaton, W. A., and Paul, B., *ApJ*, **531**, 546–552 (2000).
4. Pottschmidt, K., Wilms, J., Nowak, M. A., Pooley, G. G., Gleissner, T., Heindl, W. A., Smith, D. M., Remillard, R., and Staubert, R., *A&A*, **407**, 1039–1058 (2003).
5. Oezdemir, S., and Demircan, O., *Ap&SS*, **278**, 319–325 (2001).
6. Pottschmidt, K., Wilms, J., Nowak, M. A., Heindl, W. A., Smith, D. M., and Staubert, R., *A&A*, **357**, L17–L20 (2000).
7. Zdziarski, A. A., Poutanen, J., Paciesas, W. S., and Wen, L., *ApJ*, **578**, 357–373 (2002).
8. Scargle, J. D., *ApJ*, **263**, 835 (1982).
9. Lomb, N. R., *Ap&SS*, **39**, 447–462 (1976).
10. Benlloch, S., Wilms, J., Edelson, R., Tahir, Y., and Staubert, R., *ApJ*, **562**, L121–L124 (2001).